Hollow-Core Microstructured Optical Fiber Based Refractometer: Numerical Simulation and Experimental Studies

N. Ayyanar, G. Thavasi Raja, *Member, IEEE*, Skibina Y. S., Yashar E. Monfared, Zanishevskaya A. A., Shuvalov A. A., and Gryaznov A. Yu

***Abstract*—In this paper, we numerically and experimentally propose a novel hollow-core microstructured optical fiber (HC-MOF) biosensor for refractive index determination. The sensing mechanism of the proposed sensor is based on photonic bandgap effect and the location of transmission maxima of the fiber, which is strongly depend on the liquid analyte RI filled in the fiber core. The proposed HC-MOF biosensor demonstrates the spectral sensitivity of 5636.3 nm/RIU with a RI detection range of 1.333 to 1.3385 for different ratios of plasma in blood serum in our experimental studies. The HC-MOF proposed here can detect similar liquid analytes with RI close to 1.33. The proposed sensor with a high sensitivity, ease of operation and the possibility of real-time sensing has a strong potential for detection of liquid analytes and biomolecules with possible applications in medicine, chemistry, and biology.**

***Index Terms*—Fiber optic sensor, hollow-core microstructured optical fiber, photonics bandgap, biosensor.**

I. Introduction

LIGHT guidance in a low-index medium via photonic bandgap effect is the most important property of hollow-core microstructure optical fibers (HC-MOFs). In HC-MOFs, the micro-structured cladding of the fiber induces photonic bandgaps, and the incident light wavelengths corresponding to these bandgaps are strongly reflected by the cladding and guided in the core of the fiber [1]. HC-MOFs have been already utilized in different photonic applications including coherent light-matter interactions [2], spectroscopy [3], thermal imaging [4], supercontinuum generation [5], high power laser transmission, ultra-short lasing and pulse compression [6], [7], and efficient terahertz communications [8], [9].

Manuscript received September 15, 2021; revised November 23, 2021; accepted November 26, 2021. Date of publication January 18, 2022; date of current version April 1, 2022. *(Corresponding author: G. Thavasi Raja.)*

N. Ayyanar is with the Department of ECE, Thiagarajar College of Engineering, Madurai, Tamil Nadu 625015, India (e-mail: naece@tce.edu).

G. Thavasi Raja is with the Department of ECE, National Institute of Technology, Tiruchirappalli, Tamil Nadu 620015, India (e-mail: thavasi@nitt.edu).

Skibina Y. S., Zanishevskaya A. A., Shuvalov A. A., and Gryaznov A. Yu are with SPE LLC "Nanostructed Glass Technology," 410033 Saratov, Russia.

Yashar E. Monfared is with the Chemistry Department, Dalhousie University, Halifax, NS B3H 4R2 Canada (e-mail: y.monfared@dal.ca).

This article has supplementary downloadable material available at https://doi.org/10.1109/TNB.2022.3144313, provided by the authors.

Digital Object Identifier 10.1109/TNB.2022.3144313

On the other hand, optical fibers have been recently studied as an ideal medium for sensing different physical, chemical and biological properties of samples/mediums including temperature [10], pressure [11], mechanical strain [10], refractive index [12] and bio-concentration [13]. The main advantages of optical fiber sensors compared to conventional sensors are their small probe size, immunity to electromagnetic interference, low-cost, possibility of remote and distributed sensing and their higher detection limits. Therefore, there is a growing interest in design and fabrication of optical fiber sensors for different applications especially in liquid sensing and biosensing [13], [14]. Photonic crystal fibers (PCFs) are usually a potential candidate in such applications. One of the most important challenges of such sensors are the way you infiltrate liquid in the fiber core or air holes [15]–[17]. In order to detect a liquid sample, you have to use either an interferometric setup (which is expensive) [16] or a plasmonic material [17].

Low-index light guidance in HC-MOFs can open the field of optical fibers to new emerging research areas like gas sensing [18], and low-index liquid sensing which can have important applications in developing new biomedical instruments, analyte detection and medical diagnostic tools [19]. The most important advantages of HC-MOFs compared to regular optical fibers for liquid sensing are ease of selective liquid filling, flexibility and also a low-loss medium for light propagation using photonic bandgap effect. The first photonic bandgap-based guiding fiber was reported in [1] where the light guidance in air core of PCF at a particular wavelength was demonstrated. The possibilities of filling the hollow-core of the fiber with gasses or liquids are studied for different applications. For example, HC-MOFs have been used for gas sensing [18] and particle tracing [20].

While gas sensing and light-matter interaction inside HC-MOFs has been the center of attention in recent years, the possible applications of HC-MOFs in liquid analyte sensing, biosensing and medical applications are neglected. There were a few studies on possible application of HC-MOFs in medical applications, for example determining the concentration of cholerogenum molecules in aqueous solutions [21] or molecule-level chemical and biological detection [22] using stimulated Raman scattering inside HC-MOFs. However, as the Raman scattering effect mainly depends on the material and laser energy, the intense heating of laser beams can destroy

1558-2639 © 2022 IEEE. Personal use is permitted, but republication/redistribution requires IEEE permission.
See https://www.ieee.org/publications/rights/index.html for more information.

Authorized licensed use limited to: ULAKBIM UASL - GAZI UNIV. Downloaded on November 18,2022 at 12:28:51 UTC from IEEE Xplore. Restrictions apply.

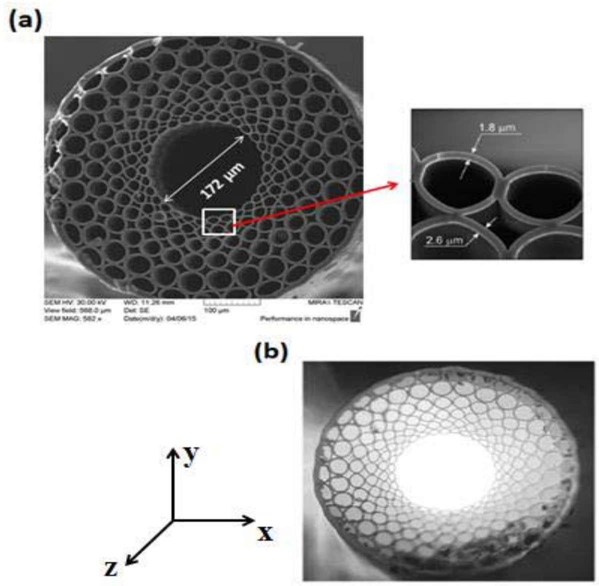

Fig. 1. (a) Scanning electron microscope (SEM) image of the cross-section of the HC-MOF used in the experiments, (b) illumination of the front facet.

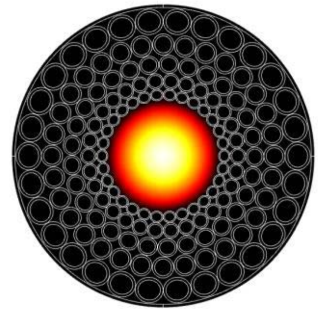

Fig. 2. The cross section and electrical field distribution of the fundamental guided mode in the proposed HC-MOF in numerical simulations using FEM with an excitation of 600 nm and the design parameters similar to the fabricated fiber.

the bio-samples and also results in low sensitivity for lower index substances.

In this work, we propose a novel and robust HC-MOF biosensor using a simple method for liquid infiltration in the main core of the fiber for biosensing and medical diagnostics applications. Using numerical simulations as well as experimental data, we demonstrate the possibility of biosensing using only the transmission spectra of the HC-MOF via the photonic bandgap effect. The HC-MOF sensor first designed using a finite element method and then fabricated using the soft glass material. The sensing performances of the fiber have been compared for different analytes (water and blood serums). We show that the maximum transmission wavelength of HC-MOF shifts with variations in bio-sample refractive index. Finally, we show that by varying the concentration of the analyte, various spectral responses can be obtained which can be used for measuring the concentration of the biomolecules in the sample.

II. Fiber Design and Fabrication

To design a sensitive biosensor, we used an HC-MOF which can demonstrate tunable photonic bandgaps based on the liquid material filled in the fiber core. The HC-MOF was fabricated by SPE Nanostructured Glass Technology (Saratov, Russia), and the details of the fabrication process of the fiber is discussed in [23]–[25]. The scanning electron microscope (SEM) image of cross-sectional view of the HC-MOF is demonstrated in Fig. 1(a).

According to Fig. 1(a), the HC-MOF consists of five concentric layers of capillaries and external buffer layer that provided structural totality in the drawing process [26]. We also included a SEM image of the illumination of the front facet of the fiber as shown in Fig. 1(b). HC-MOF is coupled with white light source at visible range of 720 nm. The diameter of the core is $d = 172\ \mu m$. The thickness of the capillary walls of each layers are $t_1 = 1.8\ \mu m$, $t_2 = 2.6\ \mu m$, $t_3 = 3.0\ \mu m$, $t_4 = 3.4\ \mu m$ and $t_5 = 4.1\ \mu m$ and filled with soft glass n = 1.519 at the wavelength of 550 *nm*. The diameters of the capillaries represent by m and n with values of five layers are $m_1 = 14\ \mu m$, $n_1 = 16\ \mu m$, $m_2 = 19\ \mu m$, $n_2 = 20\ \mu m$, $m_3 = 22\ \mu m$, $n_3 = 24\ \mu m$, $m_4 = 26\ \mu m$, $n_4 = 29\ \mu m$, $m_5 = 31\ \mu m$ and $n_5 = 35\ \mu m$, respectively as shown in the Fig. S1 (see supplementary information).The fiber preform was assembled from five circular layers of glass tubes of different diameters, each layer consisting of 30 identical cells. The ratio of inner to outer diameter of each individual tube was 0.85. Using an outer buffer layer, this structure was suspended in a cylindrical tube with a larger diameter. The entire fiber structure was made from the Russian electro-vacuum glass, which is a soft optical glass composed of 72% silica, 16% Na2O and smaller amounts of CaO, MgO and BaO. This optical glass exhibits a refractive index of 1.519 and an Abbe number V = 60, which makes its optical properties nearly identical to Schott crown glass K7. This glass was mainly chosen for its excellent thermo-elastic properties and its suitability for the fiber drawing process [27].

III. Numerical Simulations

To simulate the optical properties of the proposed HC-MOF in sensing applications, a finite element method (FEM) has been used to find the effective mode index of guided modes in the fiber core. The electric field distributions of fundamental guided mode profile for HC-MOF with 600 nm excitation wavelength through FEM analysis using COMSOL Multi-Physics software (version 5.4) is shown in Fig. 2. Note that all of the design parameters of the HC-MOF have been adopted from the fabricated structure.

In the simulations, a perfectly matched layer (PML) of 7 μm is applied to the boundary surfaces which can absorb the radiant energy and resist the reflection of any stray energy from the fiber axis. The scattering boundary condition is also applied with PML which can assist in reducing the reflected energy. Finally, a fine mesh size has been applied to the model to ensure the accuracy of the results.

IV. Experimental Setup

For biosensing setup, the optical beams transmitted to the hollow core through fiber optical cable from the optical source

Authorized licensed use limited to: ULAKBIM UASL - GAZI UNIV. Downloaded on November 18,2022 at 12:28:51 UTC from IEEE Xplore. Restrictions apply.

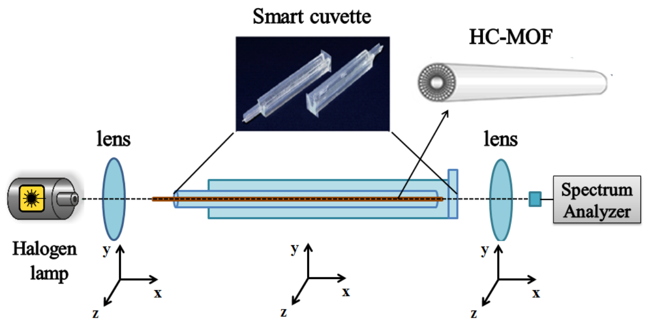

Fig. 3. The diagram of experiments for biosensing using the HC-MOF.

(halogen lamp). The light is then passed through a lens with a focal length of 6 mm. We used a collimator, attached to the two-coordinate x-y adjusting surface, to efficiently transmit the light to the fiber optic cable. The length of the proposed HC-MOF is 6.1 cm. The analyte samples are infiltrated in a special glass cuvette (smart cuvette) to be inserted inside the fiber core using a pipette dispenser. Under the action of capillary forces, the biosample (50 μl) penetrates into core of the waveguide. The quality of filling of the waveguide can be assessed visually and by the characteristic shape of the transmission spectrum. The output radiation is then collected by the second lens from the HC-MOF and is transmitted to the fiber optic cable of spectrum analyzer (Ocean Optics HR4000) which was connected to a computer via USB-interface. The schematic of the proposed biosensing setup is demonstrated in Fig. 3.

V. Sensing Performance of the Proposed HC-MOF

The transmission spectra and location of transmission peak of HC-MOF strongly depends on the geometry structure of the cladding and refractive index of the sample in the hollow core region [1]. In this study, sensing performance of two samples including blood serum for plasma detection and water is experimentally analyzed to demonstrate the possibility of biosensing using HC-MOFs and photonic bandgap guiding mechanism.

The RI of the plasma in the blood serum is measured by pocket refractometer (Atago PAL-RI) and determined to be 1.3342, 1.3346 and 1.3385 for 1/8, 1/4 and 1/2 plasma dilution with water ratios as shown in the Fig 4. The ratio of 1/2, 1/4, 1/8 is actually defined for mixture of raw plasma serum with distilled water. For example, 1/2 means 1 part of plasma serum mixed with 2 parts of distilled water. Similarly, 1/4 and 1/8 is 1 part of plasma serum mixed with 4 parts of distilled water and 1 part of plasma serum mixed with 8 parts of distilled water, respectively. The RI of water is also determined to be 1.333. Initially, we consider empty core of HC-MOF and observed transmission spectrum at the visible/NIR wavelength range of 400 nm to 900 nm as shown in Fig. 5.

The transmission spectra of experimental setup agreed very well with predicted spectra from the FEM simulations. The maximum intensity of peak wavelength is occurred around 650 nm for both experimental spectra and the spectra calculated using FEM simulations. This broad range of transmission

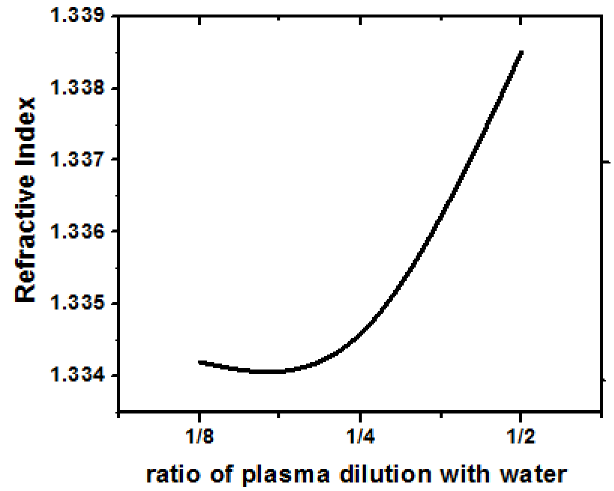

Fig. 4. Refractive index with respect to ratio of the plasma dilution with water.

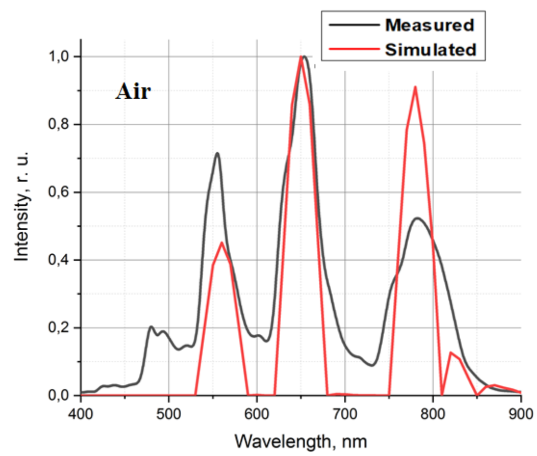

Fig. 5. Measured and simulated transmission spectrum of HC-MOF filled by air.

spectrum is more suitable for many sensing application. The obtained intensity of transmission bands depends on the size of the hollow core, cladding arrangement, and core filling material properties such as optical loss of the material and its scattering coefficients. The detailed spectral properties of HC-MOF were discussed in [23]–[25]. Similar to the previous analysis, we studied the transmission spectra of HC-MOF when the core of fiber was filled with water. A maximum intensity of peak wavelength as 626 nm for experimental and 611 nm for simulated as shown in Fig. 6. It is clear that the maximum intensity of peak wavelength is red shifted with increasing the RI of sample in the HC-MOF core. Further, sensing performance of plasma detection in blood serum is computed where hollow core filled up by blood serum. The recorded transmission power spectrum for experimental and simulation is shown in Fig. 6 for plasma sensing.

The maximum intensity of peak wavelength in experiments is determined to be 641.55 nm, 645.6 nm and 657 nm for serum 1/8, 1/4 and 1/2, respectively. The spectral sensitivity is one of the main parameters that determine the performance of a biosensor. One can easily obtain the spectral sensitivity

Authorized licensed use limited to: ULAKBIM UASL - GAZI UNIV. Downloaded on November 18,2022 at 12:28:51 UTC from IEEE Xplore. Restrictions apply.

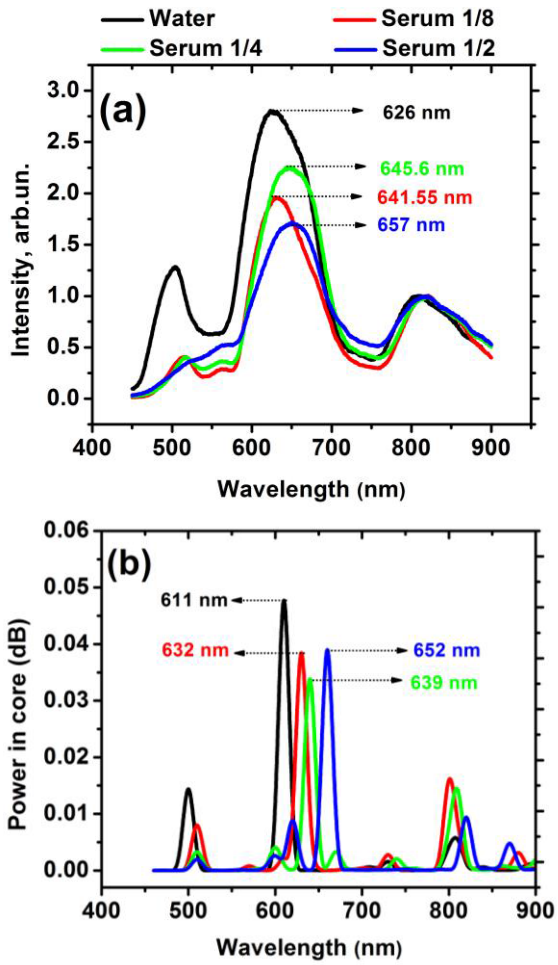

Fig. 6. (a) Experimental intensity spectra and (b) FEM simulation spectra of core guided mode power in the proposed HC-MOF with different analyte liquids filled in the core of the fiber. Note that the locations of the main peaks (peaks with the highest intensities) are used to detect a liquid analyte in the core of the HC-MOF.

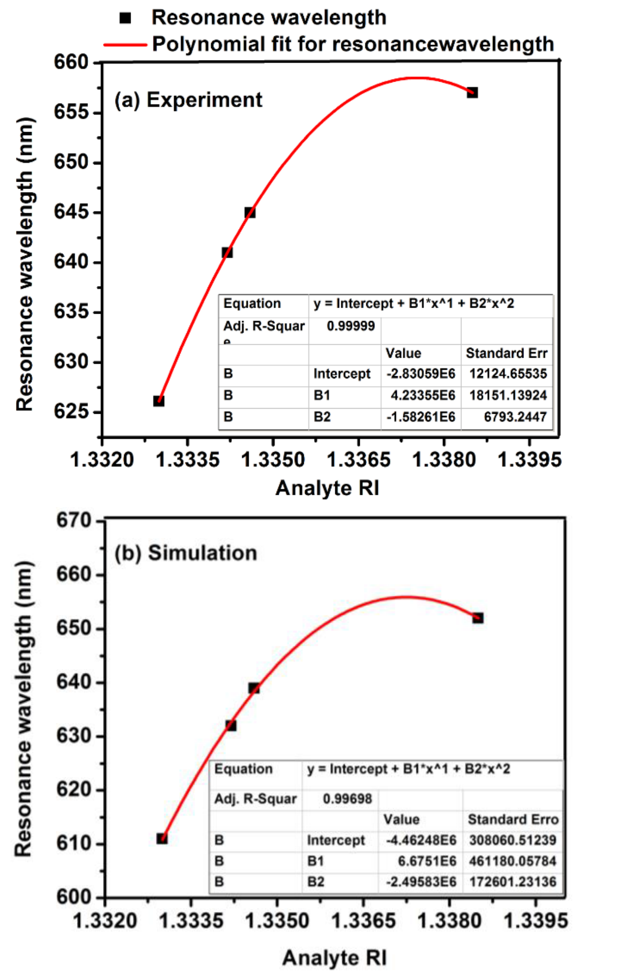

Fig. 7. Resonance wavelength (transmission peak location) of the HC-MOF as a function of analyte RI for experimental studies and FEM simulations.

of the proposed HC-MOF using the following formula [28],

$$S\ (\text{nm/RIU}) = \frac{\Delta\lambda_{peak}}{\Delta n_{analyte}}, \tag{1}$$

where, $\Delta\lambda_{\text{peak}}$ is the difference between peak wavelengths of HC-MOF spectra and $\Delta n_{\text{analyte}}$ is the difference between analyte RI of the core filling liquids. The wavelength shift for a RI change from 1.333 (water) to 1.3385 (blood serum 1/2) is equal to 31 nm in experiments and 41 nm in simulations. The shift of resonance wavelength with analyte RI for experiments and simulations is demonstrated in Fig. 7. Using Eq. 1 and Fig. 7, the spectral sensitivity of the proposed HC-MOF is determined to be 5636.3 nm/RIU for experiment and 7454.5 nm/RIU for FEM simulations with a RI detection range of 1.333 to 1.3385. Furthermore, we fitted the data points with an adjusted R-square of 0.9999 for experimental (Fig. 7 (a)) and 0.99698 for numerical (Fig. 7(b)) simulation data. The fitting equations and values are inserted in Fig. 7. According to the data in the simulations and experiments, we can detect the plasma presence in the blood serum using the proposed HC-MOF biosensor and the proposed optical setup. The high sensitivity of HC-MOF sensor together with the ease of detection, low-cost of the setup and also the possibility of real-time detection of liquid analytes can be used not only for detection of blood plasma but also for various biosensing applications and unknown analyte detection in chemistry, medicine, and biology.

The sensitivity can also discuss with both high index and lower index PCF in order to compete and prove for the proposed work has in cherish of photonics. Infact, the work based on higher index PCF [29], has good optimized structure but still they did for simulation only and that work not to be interacted with real bio samples whereas we have demonstrated real time HC waveguide with abrupt optimized structure and obtained sensitivity as 7545 nm/RIU. This range is not so far from the earlier reported PCF sensitivity value which has 9000 nm/RIU. In fact, the principle of both hollow waveguide, silica waveguide is entirely different but the effectiveness of the proposed structure is almost the reached that sensing performances of PCF. While comparing the hollow core anti resonant fiber [30], it will clearly depict that sensitivity was obtained in GHz/RIU. While analyzing the analyte value, it has higher index difference than our case but still sensitivity reached for approximately 900 GHZ/RIU with index difference of 0.005 whereas 1200 GHz/RIU for 0.06.

Authorized licensed use limited to: ULAKBIM UASL - GAZI UNIV. Downloaded on November 18,2022 at 12:28:51 UTC from IEEE Xplore. Restrictions apply.

While comparing the index difference, the proposed reach for better sensitivity at the minimal index difference.

VI. Conclusion

In conclusion, HC-MOF Refractometer was designed. The transmission power spectrums of HC-MOF were obtained through numerical simulation and experimental studies with hollow-core followed by a core filled with different liquid samples (water and blood serum). The proposed HC-MOF biosensor demonstrates the spectral sensitivity of 5636.3 nm/RIU with a RI detection range of 1.333 to 1.3385 for different ratios of plasma in blood serum in our experimental studies. We demonstrated the strong potential of our HC-MOF biosensor for detection of different liquid analytes with RI close to 1.333 which can find important applications in biomolecule detection with possible applications in medicine, chemistry, and biology.

References

[1] R. F. Cregan *et al.*, "Single-mode photonic band gap guidance of light in air," *Science*, vol. 285, no. 5433, pp. 1537–1539, Sep. 1999.
[2] Y. E. Monfared, "Transient dynamics of stimulated Raman scattering in gas-filled hollow-core photonic crystal fibers," *Adv. Mater. Sci. Eng.*, vol. 2018, Dec. 2018, Art. no. 8951495.
[3] N. Kotsina *et al.*, "Ultrafast molecular spectroscopy using a hollow-core photonic crystal fiber light source," *J. Phys. Chem. Lett.*, vol. 10, no. 4, pp. 715–720, Feb. 2019.
[4] F. Benabid, J. C. Knight, and P. J. Russell, "Particle levitation and guidance in hollow-core photonic crystal fiber," *Opt. Exp.*, vol. 10, no. 21, pp. 1195–1203, 2002.
[5] A. Ermolov, K. F. Mak, M. H. Frosz, J. C. Travers, and P. S. J. Russell, "Supercontinuum generation in the vacuum ultraviolet through dispersive-wave and soliton-plasma interaction in a noble-gas-filled hollow-core photonic crystal fiber," *Phys. Rev. A, Gen. Phys.*, vol. 92, no. 3, Sep. 2015, Art. no. 033821.
[6] G. Humbert *et al.*, "Hollow core photonic crystal fibers for beam delivery," *Opt. Exp.*, vol. 12, no. 8, pp. 1477–1484, 2004.
[7] Y. Y. Wang *et al.*, "Design and fabrication of hollow-core photonic crystal fibers for high-power ultrashort pulse transportation and pulse compression," *Opt. Lett.*, vol. 37, no. 15, pp. 3111–3113, 2012.
[8] H. Pakarzadeh, S. M. Rezaei, and L. Namroodi, "Hollow-core photonic crystal fibers for efficient terahertz transmission," *Opt. Commun.*, vol. 433, pp. 81–88, Feb. 2019.
[9] V. Sharif and H. Pakarzadeh, "Terahertz hollow-core optical fibers for efficient transmission of orbital angular momentum modes," *J. Lightw. Technol.*, vol. 39, no. 13, pp. 4462–4468, Jul. 1, 2021.
[10] Y. Wang, D. N. Wang, C. R. Liao, T. Hu, J. Guo, and H. Wei, "Temperature-insensitive refractive index sensing by use of micro Fabry–Pérot cavity based on simplified hollow-core photonic crystal fiber," *Opt. Lett.*, vol. 38, no. 3, pp. 269–271, 2013.
[11] R. E. P. D. Oliveira, C. J. S. D. Matos, J. G. Hayashi, and C. M. B. Cordeiro, "Pressure sensing based on nonconventional air-guiding transmission windows in hollow-core photonic crystal fibers," *J. Lightw. Technol.*, vol. 27, no. 11, pp. 1605–1609, Jun. 1, 2009.
[12] Z. Zhang, J. He, B. Du, K. Guo, and Y. Wang, "Highly sensitive gas refractive index sensor based on hollow-core photonic bandgap fiber," *Opt. Exp.*, vol. 27, no. 21, pp. 29649–29658, 2019.
[13] A. K. Paul, M. Samiul Habib, N. H. Hai, and S. M. Abdur Razzak, "An air-core photonic crystal fiber based plasmonic sensor for high refractive index sensing," *Opt. Commun.*, vol. 464, Jun. 2020, Art. no. 125556.
[14] S. Liu, W. Gao, H. Li, Y. Dong, and H. Zhang, "Liquid-filled simplified hollow-core photonic crystal fiber," *Opt. Laser Technol.*, vol. 64, pp. 140–144, Dec. 2014.
[15] J. Algorri, D. Zografopoulos, A. Tapetado, D. Poudereux, and J. Sánchez-Pena, "Infiltrated photonic crystal fibers for sensing applications," *Sensors*, vol. 18, no. 12, p. 4263, Dec. 2018.
[16] J. Bläsi and M. Gerken, "Multiplex optical biosensors based on multi-pinhole interferometry," *Biomed. Opt. Exp.*, vol. 12, no. 7, pp. 4265–4275, 2021.
[17] Y. E. Monfared, "Overview of recent advances in the design of plasmonic fiber-optic biosensors," *Biosensors*, vol. 10, no. 7, p. 77, Jul. 2020.
[18] F. Yang, W. Jin, Y. Lin, C. Wang, H. Lut, and Y. Tan, "Hollow-core microstructured optical fiber gas sensors," *J. Lightw. Technol.*, vol. 35, no. 16, pp. 3413–3424, Aug. 15, 2017.
[19] L. Rindorf *et al.*, "Towards biochips using microstructured optical fiber sensors," *Anal. Bioanal. Chem.*, vol. 385, no. 8, p. 1370, 2006.
[20] F. M. Cox, A. Argyros, M. C. J. Large, and S. Kalluri, "Surface enhanced Raman scattering in a hollow core microstructured optical fiber," *Opt. Exp.*, vol. 15, no. 21, pp. 13675–13681, 2007.
[21] A. V. Malinin *et al.*, "The use of hollow-core photonic crystal fibres as biological sensors," *Quantum Electron.*, vol. 41, no. 4, p. 302, 2011.
[22] X. Yang, C. Shi, R. Newhouse, J. Z. Zhang, and C. Gu, "Hollow-core photonic crystal fibers for surface-enhanced Raman scattering probes," *Int. J. Opt.*, vol. 2011, Apr. 2011, Art. no. 754610.
[23] Y. S. Skibina *et al.*, "Photonic crystal fibres in biomedical investigations," *Quantum Electron.*, vol. 41, no. 4, pp. 284–301, Apr. 2011.
[24] A. V. Malinin *et al.*, "The use of hollow-core photonic crystal fibres as biological sensors," *Quantum Electron.*, vol. 41, no. 4, pp. 302–307, Apr. 2011.
[25] D. P. Nikolelis, T. Varzakas, A. Erdem, and G. P. Nikoleli, Eds., *Portable Biosensing of Food Toxicants and Environmental Pollutants*. Boca Raton, FL, USA: CRC Press, 2013.
[26] A. A. Zanishevskaya, A. A. Shuvalov, Y. S. Skibina, and V. V. Tuchin, "Microstructured waveguides for serological examination of blood," *Proc. SPIE*, vol. 9448, Mar. 2015, Art. no. 944807.
[27] J. S. Skibina *et al.*, "A chirped photonic-crystal fibre," *Nature Photon.*, vol. 2, no. 11, pp. 679–683, Nov. 2008.
[28] Y. Esfahani Monfared, "Refractive index sensor based on surface plasmon resonance excitation in a D-shaped photonic crystal fiber coated by titanium nitride," *Plasmonics*, vol. 15, no. 2, pp. 535–542, Apr. 2020.
[29] A. Kumar Paul, A. Krishno Sarkar, A. B. S. Rahman, and A. Khaleque, "Twin core photonic crystal fiber plasmonic refractive index sensor," *IEEE Sensors J.*, vol. 18, no. 14, pp. 5761–5769, Jul. 2018.
[30] J. Sultana *et al.*, "Hollow core inhibited coupled antiresonant terahertz fiber: A numerical and experimental study," *IEEE Trans. Terahertz Sci. Technol.*, vol. 11, no. 3, pp. 245–260, May 2021.

Authorized licensed use limited to: ULAKBIM UASL - GAZI UNIV. Downloaded on November 18,2022 at 12:28:51 UTC from IEEE Xplore. Restrictions apply.